SUPPLEMENTARY INFORMATION

Enhancing the Sensitivity of Label-free Silicon Photonic Biosensors through Increased Probe Molecule Density

*Shuren Hu, Yiliang Zhao, Kun Qin, Scott T. Retterer, Ivan I. Kravchenko and Sharon M. Weiss**

**E-mail: sharon.weiss@vanderbilt.edu*

S1: Target concentration-dependent sensor response

Silicon micro-ring resonators functionalized with either in-situ synthesized ssDNA probe molecules or directly conjugated ssDNA probe molecules were exposed to a variety of concentrations of target ssDNA and target ssPNA molecules. No change in the magnitude of the resonance wavelength shift of the sensors was observed when the target ssPNA concentration was varied between 1-100 μM. A concentration-dependent resonance shift was observed when the target ssDNA concentration was varied between 10-100 nM, as shown in Figure S-1. Note that the resonance shifts measured for sensors exposed to 100 nM target ssDNA molecules are only slightly less than those shown in Figure 3 in the main text for 100 μM concentration, suggesting that nearly all probe molecule binding sites are saturated when exposed to at least 100 nM concentration of target molecules. Micro-ring resonators functionalized with in-situ synthesized ssDNA probe molecules could detect down to 10 nM target ssDNA concentration while sensors functionalized with directly conjugated ssDNA probe molecules could detect down to 50 nM target ssDNA. Since the target molecule concentration in solution decreases as the target molecules are hybridized to ssDNA probe molecules, for ultra-low concentration detection, it is important to reduce the non-transducable area on the sensor surface. In the experiments presented in this work, the entire silicon chip surface was functionalized with probe molecules. Therefore, most of the target molecules in low concentration solutions are bound to regions of the chip that do not overlap with the resonant mode of the ring resonators and photonic crystals and thus do not contribute to a shift of the resonance wavelength. Assuming that target molecules uniformly bind onto surfaces across the silicon chip, it is possible to estimate the sensor detection limit based on the area ratio between the device region (i.e., micro-ring) and the entire silicon chip. The ring resonators are 5 μm in radius with 500 nm wide waveguides. The size of the silicon chip is approximately 5 mm by 5 mm. Accordingly, this means that only 0.00006% of the total number of bound target molecules contribute to a resonance shift in our sensors. For in-situ functionalized samples, the detection limit could be as low as 6 fM, while the detection limit of ring resonators prepared by the conjugation method could be as low as 31 fM if only the ring resonator region was exposed to target molecules.

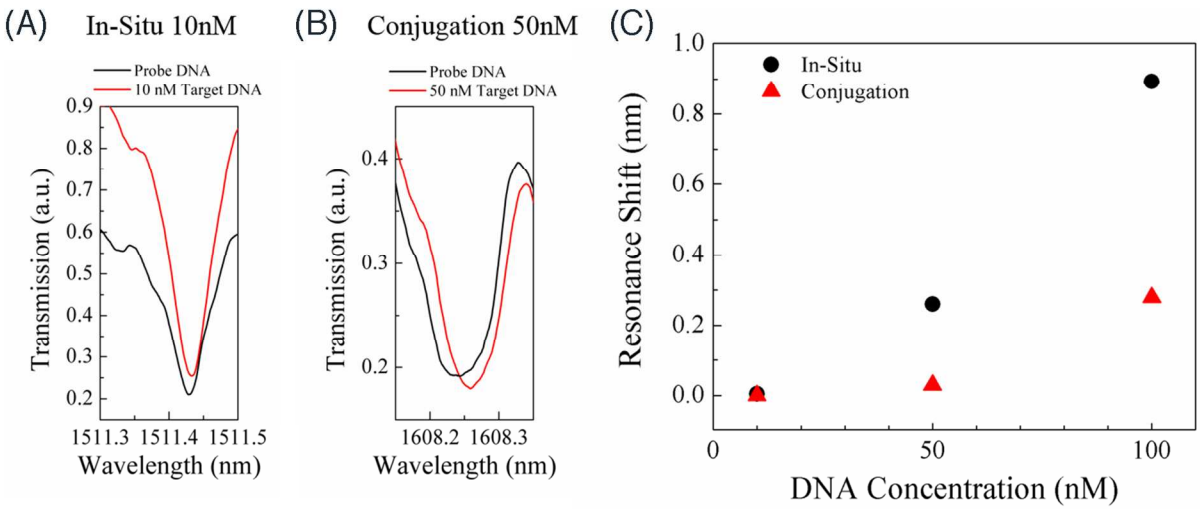

Figure S1 (A) Resonance shift (0.005 nm) when 10 nM target ssDNA is exposed to a micro-ring resonator functionalized with in-situ synthesized ssDNA probe molecules. (B) Resonance shift (0.02 nm) when 50 nM target ssDNA is exposed to a micro-ring resonator functionalized with directly conjugated ssDNA probe molecules. (C) Comparison of resonance shifts at different target ssDNA concentrations for both in-situ and conjugation prepared sensors.

S2: Saturation of probe coverage by conjugation method

The probe density resulting from the conjugation functionalization method described in the main text was further explored by examining different probe attachment conditions, including varying the ion strength in buffer solution, varying the probe attachment time, and varying the probe solution concentration. The results for ion strength and attachment time are discussed below. For sensors tested with ssDNA probe attachment with concentrations of 10 μM, 20μM, 50μM and 100 μM in an excess volume of incubation solution (> 200μL solution), the resulting resonance wavelength shifts were all consistent and did not show any dependence on the probe solution concentration.

S2-1: Varying the ion strength in ssDNA probe solution

It has been demonstrated that when using a traditional ssDNA conjugation method, steric hindrance can be mitigated by increasing the ion strength in the probe ssDNA solution, for example by adding $MgCl_2$ into the probe solution. In order to investigate whether adding $MgCl_2$ into the ssDNA probe solution could affect the resulting resonance shift, three chips with four micro-ring devices each were functionalized in probe solutions with different $MgCl_2$ concentration using the traditional conjugation method. As shown in Figure S2-1, the resonance wavelength shift increased slightly when $MgCl_2$ was added to the probe solution with the shift saturating for $MgCl_2$ concentrations above 50 mM. However, the resulting resonance shift (0.35 nm) is much less than that of micro-rings functionalized using in-situ synthesized probe molecules (1.3 nm).

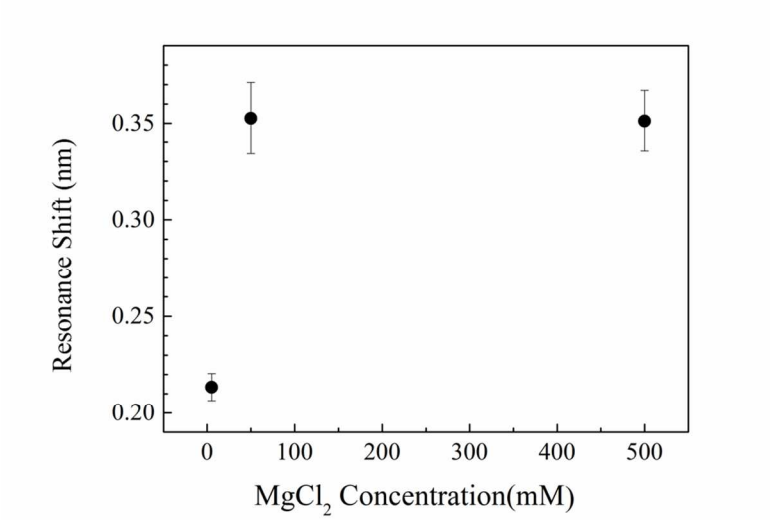

Figure S2-1. Micro-ring resonator resonance shifts after ssDNA probe attachment in different $MgCl_2$ concentrations. Three concentrations were tested: 5 mM, 50 mM and 500 mM. The resonance shift is saturated for a $MgCl_2$ concentration of 50 mM, implying a saturation of the probe surface coverage by the conjugation method.

S2-2: Varying the probe ssDNA attachment time

In order to determine whether longer ssDNA probe incubation times increased the number of bound probe molecules, the probe attachment time was varied from 1-12 hours, as shown in Figure S2-2. The 12 hour ssDNA attachment results in only a slight increase (~6%) of the resonance wavelength shift on average, implying that the probe surface coverage is nearly saturated after one hour incubation.

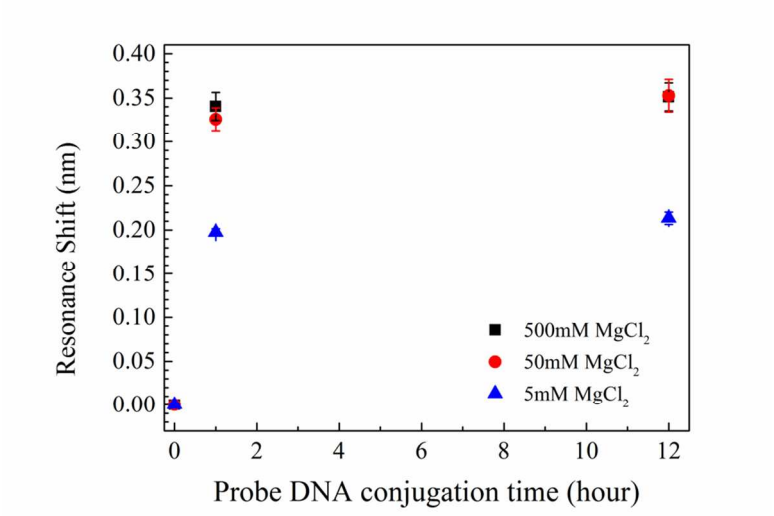

Figure S2-2. Micro-ring resonator resonance shifts after probe attachment for different incubation times. After 12 hours incubation, the average resonance shift only increases by 6%.

S3: Control experiments

The robustness of the surface functionalization methods used in this work was evaluated by testing for non-specific binding events. Two different types of non-specific binding events were considered: ssPNA target molecules attaching to the sensing surface in the absence of complimentary ssDNA probes and non-complementary ssPNA sequences non-specifically binding to surface immobilized ssDNA probes. **Figure S3a** shows the negative control test results for a ring-resonator prepared to be functionalized by in-situ ssDNA probe synthesis. After silanization with TEOS-HBA and before ssDNA probe synthesis, the sample was incubated in a 100 µM ssPNA target solution. Negligible resonance wavelength red-shift (~0.034 nm) was detected verifying that ssPNA target sequences do not bind to the sensing surface in the absence of complementary ssDNA probe sequences. After carrying out in-situ ssDNA probe synthesis (5'-GGT TCC GAA CGG AGA C-3'), the sample was then exposed to a 100 µM solution containing a completely mismatched ssPNA sequence (ACG AGG ACC ATA GCT A) in DI water. Almost no red-shift (~0.002 nm) of the resonance wavelength was detected confirming the absence of non-specific binding of the mismatched ssPNA sequence to in-situ synthesized ssDNA probe molecules. **Figure S3b** shows the negative control test results for a ring-resonator prepared to be functionalized by the direct conjugation method of ssDNA probe attachment. A negligible resonance red-shift (~0.008 nm) was measured after exposure of ssPNA target molecules to the ring containing silane and linker surface species but no ssDNA probe molecules. After ssDNA probes were conjugated to the sensing surface (same sequence as synthesized probes), the sample was incubated in a 100 µM solution containing completely mismatched ssPNA target in DI water (ACG AGG ACC ATA GCT A). The very small resulting resonance red-shift (~0.018 nm) verifies that non-complimentary nucleic acid sequences will not bind to the conjugated ssDNA probe molecules.

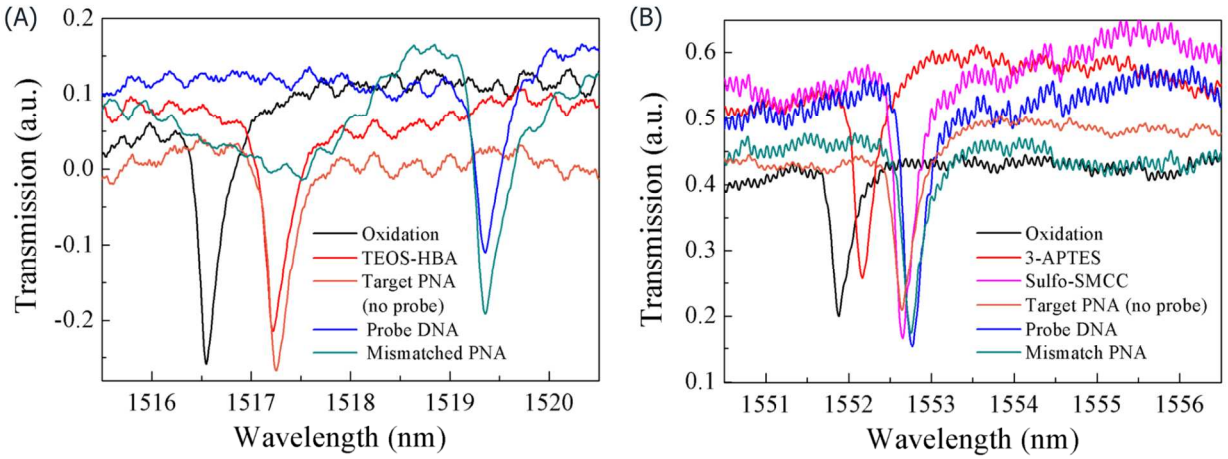

Figure S3. Control experiments demonstrating the absence of non-specific binding for ring resonators functionalized using (a) the in-situ ssDNA probe synthesis method and (b) the direct conjugation method of ssDNA probe attachment, as described in the text above.

S4: Characterization of fluorescently-tagged ssDNA

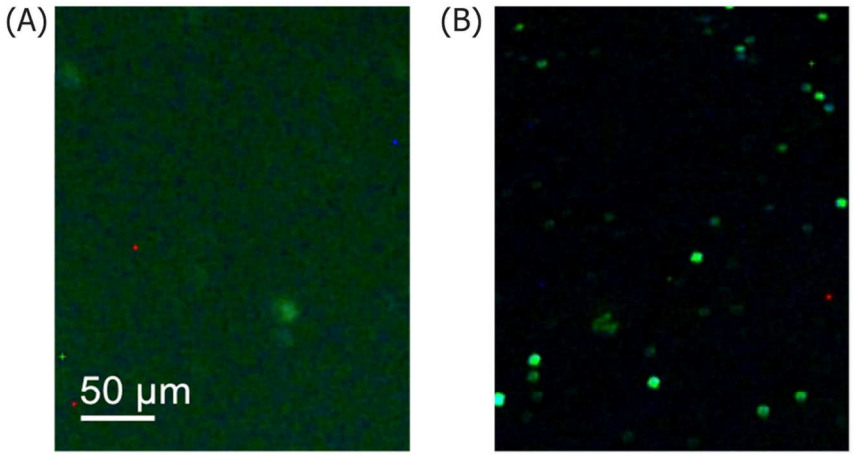

Figure S4-1. Fluorescence images of substrates prepared with (a) in-situ synthesized and (b) directly conjugated FAM6-labeled fluorescent ssDNA.

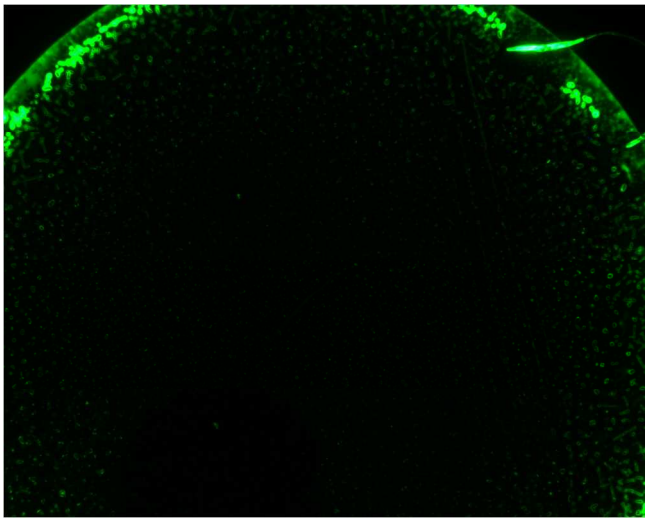

Figure S4-2. "Coffee ring" effect of drop-cast FAM6-labeled fluorescent ssDNA on silicon surface as imaged in a fluorescence microscope.

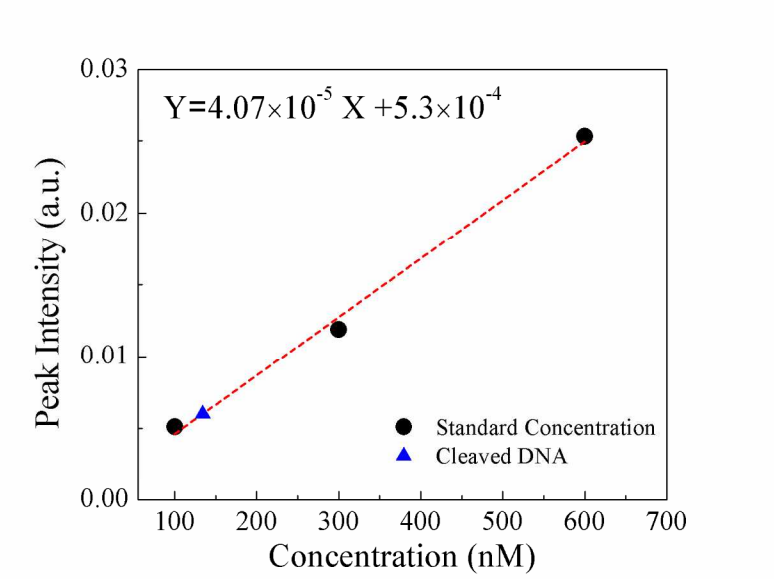

Figure S4-3. Calibration curve linking peak absorbance intensity measured at the characteristic absorption peak of the FAM6 dye to known concentrations of FAM6-labeled ssDNA in solution. A linear fit of the data and associated equation are shown. Based on comparison to this data, the concentration of ssDNA cleaved from a silicon sample functionalized by the direct conjugation approach with a cleavable linker is estimated to be 134 nM.

S5: Scheme for cleaving ssDNA probes from silicon surface

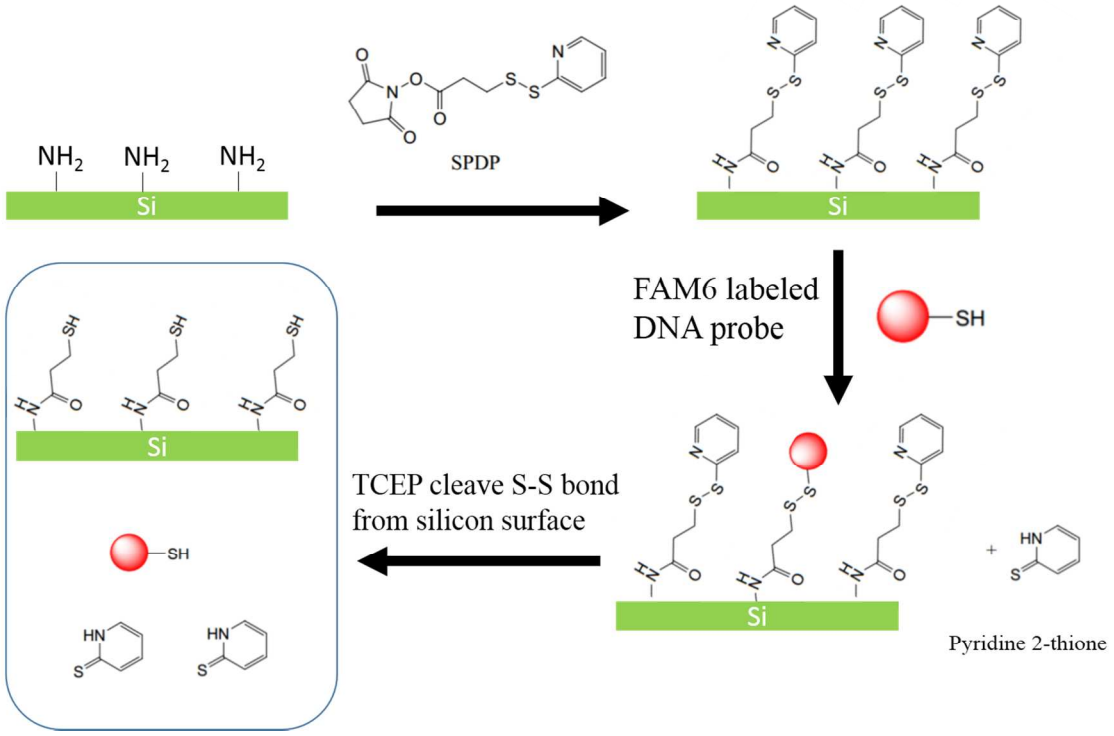

Figure S5-1. Schematic representation of the steps involved in cleaving FAM6-labeled ssDNA from an amine-terminated (3-APTES) silicon surface following covalent immobilization through the cleavable SPDP linker molecule. Complete details are found in the Methods section in the main text. Briefly, SPDP is attached to 3-APTES on the silicon surface. FAM6-labeled ssDNA probe molecules are then attached to the SPDP linkers. Pyridine 2-thione groups on the SPDP molecules are displaced when the ssDNA is attached. Next, a TCEP solution is used to cleave the SPDP molecules, releasing the FAM6-labeled probe DNA into solution. Pyridine 2-thione is also present in the solution since not all SPDP sites capture a ssDNA probe molecule. The concentration of ssDNA probe molecules and pyridine 2-thione can be determined by measuring the absorbance at 495 nm and 343 nm, respectively.

S6: Microfluidic Flow Cell Fabrication

A mold of the flow cell is formed by optical lithography on a 100 µm thick SU-8 layer (SU-8 2100) on a 4-inch silicon wafer. A mixture of PDMS and curing agent (10:1) was poured onto the surface of the mold to form a PDMS flow cell which was cured in an oven at 60℃ for 4 hours. The cured PDMS flow cell was then carefully peeled off the mold and cut out using a graver. An 18 gauge punch was used to make holes at each end of the channel for the inlet and outlet. To achieve optimized adhesion, the bottom surface of the PDMS flow cell was treated with oxygen plasma for 25 s, and then an adhesive curing glue (a 2:1 mixture of PDMS and curing agent) was uniformly applied. The PDMS flow cell channel was then aligned with the silicon photonic devices (rings or photonic crystals) under an optical microscope and attached to the silicon-on-insulator (SOI) substrate. Next, the SOI substrate and PDMS flow cell were clamped and cured in an oven for 4 hours at 60°C. Finally, two connection pins (outside diameter 16 gauge) with tubing were plugged into the inlet and outlet of the PDMS shell.

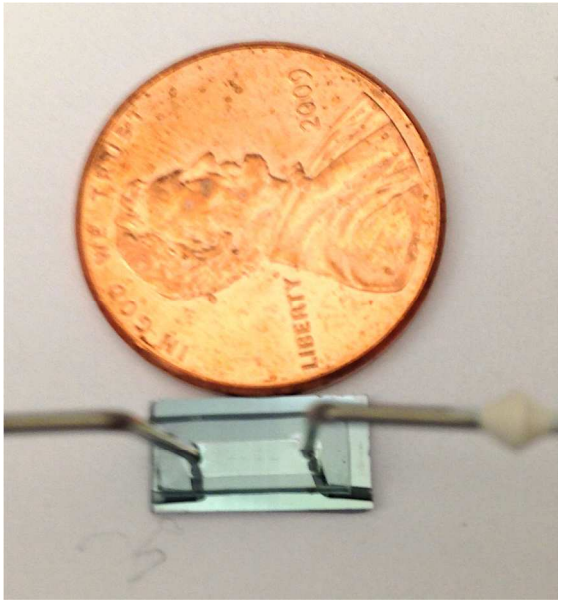

Figure S6. Photograph of microfluidic channel integrated with silicon micro-ring resonators.